Numerical Studies on Design of Terfenol-D Actuator using Coaxial Coils

Raghavendra Joshi
Faculty & PG Co-ordinator
Department of Mechanical Engineering
Ballari Institute of Technology & Management, Bellary

ABSTRACT
Attaining a controlled output strain and utilizing a full potential of active material are the significant factors to design Terfenol-D actuator devises such as active damping devices, high speed hydraulic valve actuators, large-force linear motors and large torque rotating motors. To achieve this, a high magnetic biasing field is required in an actuator. The present work attempts to propose a suitable layout in a Terfenol-D actuator based on numerical magnetic field analysis. Three configurations namely single coil, coaxial coils and coil with permanent magnet combinations that surrounds the Terfenol-D material are considered in the present study. Ansoft package magnetic flux density is used to evaluate the distribution of magnetic flux density of the layouts used in an actuator. Further, the magnetic flux density is evaluated and compared among them to decide the best configuration to be used in a Terfenol-D actuator. Structure and layout of a proposed actuator is outlined. With this, the number of turns required for coaxial coils is computed using Ampere's law and in turn verified the same using the reluctance approach. Finally, it appears that all these results work as well as anticipated and has their individual advantages.

Keywords
Terfenol-D, Biasing, Magnetic flux density, Ansoft, Coaxial coils, Permanent magnet, Ampere's law, Reluctance approach.

1. INTRODUCTION
Terfenol-D is a new kind of functional material driven by magnetic field. It is an alloy containing terbium (Tb) and dysprosium (Dy) with iron (Fe). Terbium generates strains, dysprosium minimizes the field strengths required to generate the strains and iron allows the alloys exceptional transduction properties to be used at or above room temperature. The devices made of this material needs low voltage input level and can produce giant" magnetostriction i.e. a strain greater than the most available commercial smart materials. To attain more magnetostriction, the selection of suitable configuration that surrounds the Terfenol-D is required. Extensive research is carried and still on by many researchers to achieve the desired output from the actuator using Terfenol-D. Analysis has been conducted using Maxwell solver, FEM, COMSOL multiphysics to improve intensity and uniformity of the magnetic field by incorporating appropriate and essential arrangement in an actuator. An extensive computer modeling using finite element method on a basic actuator with different magnetic circuit configurations [1], closed magnetic structure has been proposed and optimized with different magnetic circuit structure for on-off type GMA [2], multi-scale external concavity structure model has been proposed [3], relation between the GMM actuator coils and the magnetic field intensity of GMM rod with both DC and AC input supply [4], the radial distribution of internal magnetic field intensity [5], the radial distribution rules of internal stress and strain on Terfenol-D [6], magnetic circuit analysis for acoustic vibration element [7], optimal design method for low consumption type DC solenoid actuator used in automobile and aircraft [8], equivalent magnetic circuit equation to optimize the electromagnetic performance [9], static magnetic field distribution has been investigated using COSMOSM program finite element package [10], integrated optimized design (includes magnetic and thermal design) method using finite element analysis [11], good agreement has been yielded on comparing the results of magnetic field simulation using FEMM software package and experimental measurements of the magnetic flux density [12] and the driving coil's structure has been designed and its shape was optimized on G-factor with the electromagnetic field analysis function available in ANSYS to ensure homogeneous magnetic field along the magnetostrictive rod. The objective of the paper is to suggest best suitable configuration by considering the three different configurations that surrounds the active material in an actuator using Ansoft analysis.

2. TYPES OF LAYOUT USED IN A TERFENOL-D ACTUATOR
Magnetostriction of a Terfenol-D depends on the type of layouts used in a Terfenol-D actuator. Four different types of layouts are TC (Terfenol-D, Coil) layout, TCM (Terfenol-D, Coil, Permanent Magnet) layout, TMC (Terfenol-D, Permanent Magnet, Coil) layout and MTC (Permanent Magnet, Terfenol-D, Coil) layout and its features as shown in Table 1. Each layout has its own advantages and disadvantages. TC and TCM layouts are simple in construction and cost effective with high energy density apart from more eddy current losses. Eddy current losses are varying in different layouts that yield different output from the Terfenol-D actuator.

3. MAGNETIC FIELD ANALYSIS OF A DIFFERENT CONFIGURATIONS
The combination of coil with permanent magnet or single coil applying a dc bias field superimposing with an alternating field is most often used layouts in a Terfenol-D actuator. In addition, a combination comprising two coaxial coils are used in the present work. These three configurations are analyzed numerically the distribution of magnetic field using Maxwell 2D solver. To explore the possible differences among these configurations, the numerical analysis is presented using these three arrangements in an actuator. Single coil of 1000 turns, coaxial coils i.e. coil 1 and coil 2 equal to 560 and 440 turns, and single coil of 1000 turns with permanent magnet are the three combinations that surrounds the Terfenol-D is considered. In each case, the direct current input of 4 A is supplied. Single coil of size (inner and outer radii are 16.5 mm and 57.5 mm respectively), single coil with permanent magnet of same size and coaxial coils (inner and outer radii of

coil 1 are 16.5 mm and 36.5 mm, coil 2 are 37.5 mm and 57.5 mm) axi-symmetric models were built separately in the Ansoft environment in free air. Suitable materials i.e. copper material for coils and Alnico for permanent magnet have been assigned and energized with current density corresponding to 4 A. The current density for single coil is 1175 kA/m^2 and for coaxial coils i.e. for coil 1 and coil 2 are 1350 and 1030 kA/m^2 respectively. The input to the permanent magnet is 4 A dc input with material properties like magnetic retentivity and magnetic coercivity of 1.27 Tesla and 50 kA/m respectively (material database from Maxwell 2D). Three models in free air alone are solved using Ansoft Maxwell 2D solver to evaluate magnetic flux density.

3.1 Comparison of magnetic flux density

The comparison of magnetic flux density obtained for single and coaxial coils, coaxial coils and single coil with permanent magnet in free air is shown in Figure 1 and 2. Maximum flux density of 45 mT is achieved from both single and coaxial coils in free air. Axial flux density distribution was uniform with coaxial coils, whereas it was disorder with single coil. The reason may be due to flux leakage during the magnetic transduction from a single coil at few points along the axial direction.

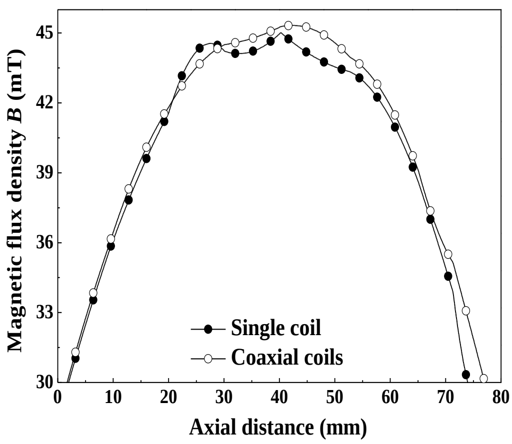

Fig 1: Numerical magnetic flux density of single and coaxial coils in free air

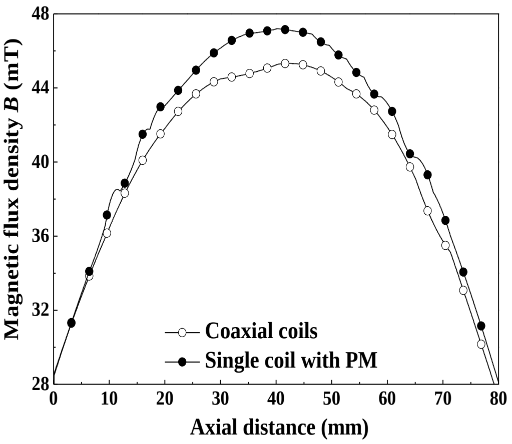

Fig 2: Numerical magnetic flux density of coaxial coils and single coil with permanent magnet in free air.

Maximum flux density of 47 mT is observed for single coil along with a permanent magnet compared to coaxial coils in free air. The distribution of flux density along the axial direction with coaxial coils is uniform, though the magnitude of flux is little higher in a single coils with permanent magnet compared to a coaxial coils of 45 mT. It is recapitulated that the enormity of flux density with all the three configurations are roughly same for a given input of 4 A. Nevertheless, the circulation of flux density along the axial direction in coaxial coil configuration is symmetrically distributed compared to single coil alone and as well as single coil with permanent magnet configuration. With this, it is accomplished that the coaxial coils using in the actuator will donate successfully good actuation force with equal density compared to single coil and as well as single coil with permanent magnet. The axi-symmetric model, model discretized with triangular finite elements and convergence data for each configuration is shown in Figure 3 to 5. Further, this analysis gave way to propose a Terfenol-D surrounded by coaxial coils configuration, together enclosed in a cylindrical housing.

4. LAYOUT AND MAGNETIC CIRCUIT OF A PROPOSED ACTUATOR

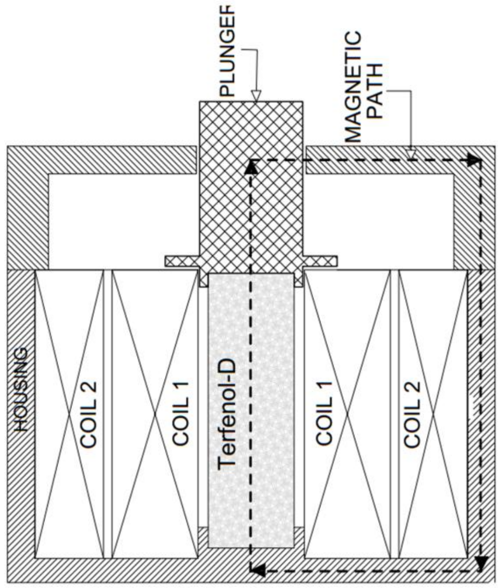

Fig 6: Structure and layout of a Terfenol-D actuator

The design of actuator has been carried out based on known dimensions of Terfenol-D with a diameter of 28 mm and length of 80 mm and requirement of magnetic field. Figure 6 shows the proposed configuration of a Terfenol-D actuator. Here, the Terfenol-D is surrounded by the coaxial coils namely coil 1 and coil 2. By supplying direct current to coil 1 a bias magnetic field will be generated and helps to attain linear response, and over which is superimposed the magnetic field strenght produced by coil 2 under direct current or alternating current input. The Terfenol-D rod and coaxially placed coils are enclosed in a chlindrical housing made up of ferromagnetic material such as mild steel. The magnetic circuit of an proposed actuator is composed of other components like aluminium bobbin and plunger. The end effect and magnetic leakage are unavoidable as the axial length and diameter of coils is finite. This yields the inhomogeneous driving magnetic field. Therefore, the length of coils should be chosen slightly longer than the Terfenol-D, which results in the active material being surrounded by homogeneous magnetic field. A closed magnetic circuit is to be adopted to reduce the flux leakage from the coils.

4.1. Number of turns for coaxial coils

The main source of magnetic field is coil 1 and coil 2 and the magnetic field strength will depend on number of turns in each coil. Magnetostriction curves available for different pre-stress against the applied field [13] were referred to decide the magnetic field intensity to be produced from coaxial coils. The linear behaviour of Terfenol-D material was found at an applied field ranging from 48 kA/m (603 Oe) to 52 kA/m (654 Oe), and the corresponding magnetostriction is 1000 -1800 ppm for an optimum prestress of 6.9 MPa. Magnetic field strength of 28 kA/m and 22 kA/m from coil 1 and coil 2 is fixed by choosing average field of 50 kA/m. Maximum magnetic field is to be produced from coil 1 as it is used for biasing the magnetic field. The reason is that the biasing linearizes and improves the performance of a Terfenol-D actuator. Terfenol-D rod and hollow cross-sectioned coaxial coils in an actuator layout together forms a conductor carrying a current for which Ampere’s law was used to find number of coil turns. According to Ampere’s law, number of turns required for coil is given by:

$$N_{coil} = \frac{H_{coil} l_{coil}}{I} \quad (1.1)$$

Where the magnetic field produced by the coil is H_{coil} , l_{coil} is length of coil, N_{coil} is the number of turns in a coil and I is the current input to coil. The number of turns for coil 1 and coil 2 are 560 and 440 for producing 28 and 22 kA/m using 4 A.

4.2. Verification of number of coaxial turns using reluctance approach

Figure 7 shows the main magnetic path through the Terfenol-D actuator. There are eight designated section through which the magnetic flux passes. For each section, there is length of magnetic path (l) and a value for the magnetic field (H). The length is fixed by geometry of the magnetostrictive actuator but the magnetic field (H) is calculated by use of the magnetic properties of the material. The material for actuator housing, top end plate, bottom end plate and plunger is mild steel. Let, $\Re_1$ = reluctance offered by Terfenol-D rod, $\Re_2$ = reluctance offered by plunger, $\Re_3$ = reluctance offered by top end plate, $\Re_4$ = reluctance offered by top end plate edge, $\Re_5$ = reluctance offered by housing thickness, $\Re_6$ = reluctance offered by bottom end plate edge, $\Re_7$ = reluctance offered by bottom end plate and $\Re_8$ = reluctance offered by bottom support of Terfenol-D.

The reluctance $\Re$ in the magnetic circuit is analogous to resistance in electric circuit. The simple equation for calculating the reluctance of circuit is given by,

$$\Re = \frac{NI}{\phi} \quad (1.2)$$

Therefore the number of turns is given by,

$$N = \frac{\Re \mu_0 \mu_{r(Terfenol-D)} H_{Terfenol-D} A_{Terfenol-D}}{I} \quad (1.3)$$

Where $\Re$ = Total reluctance of magnetic circuit equal to $\Re = \Re_1 + \Re_2 + \Re_3 + \Re_4 + \Re_5 + \Re_6 + \Re_7 + \Re_8$.

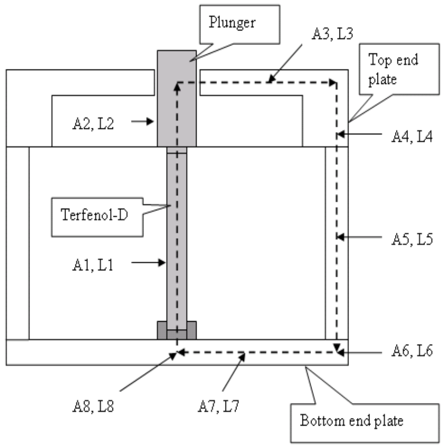

Fig 7: Magnetic flux path in a Terfenol-D actuator

The individual reluctance along the path can be calculated by using equation

$$\Re = \frac{l_i}{\mu_0 \mu_r A_i} \quad (1.4)$$

Where l_i = length of section of component,

A_i = cross sectional area of the component.

i = 1, 2, 3 ...8.

Reluctance of each component is calculated using Eq. (1.4) and is tabulated in Table 2. Number of turns for coaxial coils is calculated using Eq. (1.3). With this number of turns for coil 1 and coil 2 are 560 and 440 to produce 28 kA/m and 22 kA/m respectively. It is evident that the number of coil turns calculated using Ampere’s law and reluctance approach are same.

5. CONCLUSION

A method to design biased Terfenol-D devices has been presented. Based on magnetic field analysis, three configurations used in the present work have its advantages and disadvantages. However, it is summarized that the good bias excitation system should use a coil bias which does not store dynamic magnetic energy. A good system should also avoid non-uniform magnetic fields in Terfenol-D and flexure in mechanical items. The proposed Terfenol-D actuator with coaxial arrangement has a high strain capability, good coupling factor of around 53 %, simplicity of construction and good efficiency. Number of turns is 560 and 440 for coil 1 and coil 2 to produce the required magnetic field. The verification of the same using reluctance approach suggests that the actuator is well suitable to predict the desirable output. Based on the analysis of magnetic field, the proposed actuator can be designed and fabricated. Experiments can be carried out to measure the output magnetostriction of Terfenol-D actuator under AC and DC excitation. The output can be enhanced by coupling the actuator unit to either mechanical or hydraulic amplifying unit. Further, the coupled unit can be used in certain applications are the future scope of the present work.

6. ACKNOWLEDGMENTS

Our thanks to the Mukund Patil and M. Subba Rao, PG students of NITK, Surathkal who have given inputs to carry out successfully the numerical analysis using Ansoft software.

7. REFERENCES

[1]. Benbouzid, M. E. H., Reyne, G. and Meunier, G (1995). "Finite element modeling of magnetostrictive devices: Investigation for the design of the magnetic circuit." IEEE transaction on Magnetics, 31(3), 1813-1816.

[2]. Li, L., Zhang, C., Yang, B. and Li, X. (2007). "Finite element analysis of the uniformity magnetic field for on-off giant magnetostrictive actuators." *International Conference on Electrical Machines and Systems* (ICEMS), 17-20th October, Wuhan, China, 3758-3761.

[3]. Wang, L., Ye, H., Liu, Y. T. and Yao, S. M. (2006). "Analysis and optimization for uniformity of magnetic field during the giant magnetostriction." Journal of Physics, 48, 1336-1340.

[4]. Han, H., Xin, Q. and Wang, S. (2008). "Finite element analysis on magnetic field in the actuator of giant magnetostrictive linear motor with Ansoft." *IEEE International Conference on Industrial Technology*, Chengdu, 1-5.

[5]. Wang, J., Li, G., Wang, C. and Liu, C. (2011a). "Finite element analysis of internal magnetic field on Terfenol-D rod in high frequency driven." *International Conference on Artificial Intelligence, Management Science and Electronic Commerce*, 5572-5575.

[6]. Wang, C., Wang, J. and Li, G. (2011b). "Finite element analysis of internal stress and strain on Terfenol-D rod in high frequency driven." *International Conference on Artificial Intelligence, Management Science and Electronic Commerce*, 5576-5579.

[7]. Wakiwaka, H., Umezawa, T. and Yamada, H. (1993). "Improvement of flux density uniformity in giant magnetostrictive material for acoustic vibration element." *Proceedings of IEEE, Transaction on Magnetics*, Nagano, Japan, 29(6), 2443-2445.

[8]. Sung, B. J., Lee, E. W. and Lee, J. G. (2007). "A design method of solenoid actuator using empirical design coefficients and optimization technique." *IEEE International Conference on Electric Machines and Drives*, 1, 279-284.

[9]. Dehui, L., Quanguo, L. and Yuyun, Z. (2008). "Magnetic circuit optimization design of Giant magnetostricitve actuator." *9th International Conference Computer-Aided Industrial and Conceptual Design (CAID/CD)*, 22-25th November, Kunming, 688-692.

[10]. Bansevicius, R. and Virbalis, J.A. (2008). "Investigation of magnetic circuit permanent magnet-Terfenol-D-Air."

Electronics and Electrical Engineering, 86, 1-6.

[11]. Lu, Q., Jing, C., Min, Z. and Dingfang, C. (2010)."Integrated optimized design of GMA with double water-cooling cavums." *International Conference on Mechanic Automation and Control Engineering*, 26-28th June, Wuhan, 3562-3565.

[12]. Olabi, A. G. and Grunwald, A. (2008). "Computation of magnetic field in an actuator." Simulation Modeling Practice and Theory, 16, 1728-1736.

[13]. Engdahl, G. (2000). "Handbook of Giant Magnetostrictive materials," *Royal Institute of Technology, Stockholm*, Sweden, 1-340.

8. APPENDIX

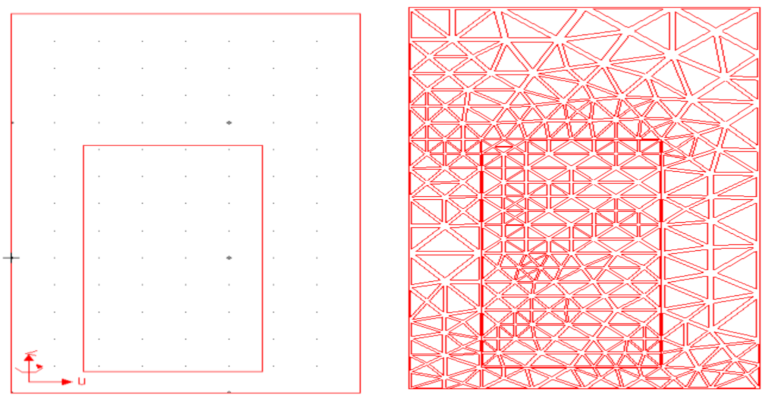

(a) **(b)**

CONVERGENCE DATA

Number of passes:
Completed 11
Remaining 0

Convergence criteria:
Target Error: 1%
Energy Error: 14.3%
Delta Energy: 0.135%

Pass	Triangles	Total Energy(J)	Energy Error(%)	Mag Force(N)
1	24	2.68925E-001	202.9396	4.93072E-001
2	65	2.43383E-001	31.4945	3.16436E-001
3	83	2.40838E-001	24.6697	2.67149E-001
4	107	2.39946E-001	22.7787	2.31003E-001
5	135	2.37665E-001	20.6925	2.15624E-001
6	174	2.36240E-001	17.0261	2.38557E-001
7	222	2.35594E-001	15.8037	2.50390E-001
8	286	2.35251E-001	15.6643	2.30816E-001
9	365	2.35700E-001	14.6039	2.41176E-001
10	469	2.35144E-001	14.4139	2.44114E-001
11	607	2.34828E-001	14.2539	2.51242E-001

(c)

Fig 3: (a) Axi-symmetric model (b) discretized with triangular elements and (c) convergence data of a single coil in free air

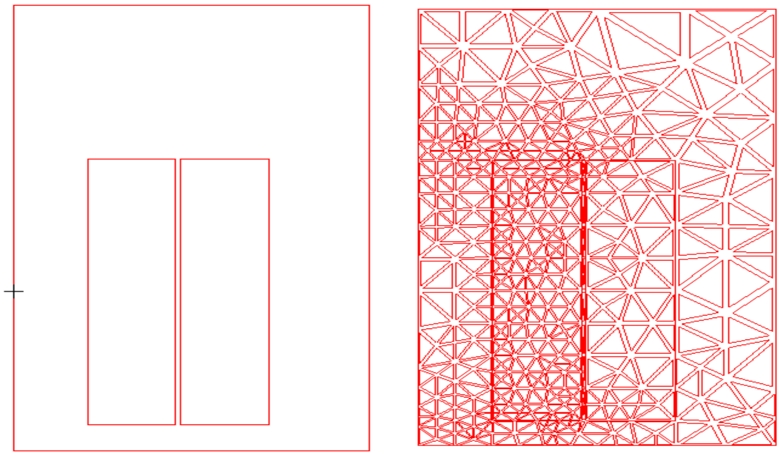

(a) (b)

CONVERGENCE DATA

Number of passes:

Completed 10

Remaining 0

Convergence criteria:

Target Error: 1%

Energy Error: 9.16%

Delta Energy: 0.0938%

Pass	Triangles	Total Energy(J)	Energy Error(%)	Mag Force(N)
1	34	1.86011E+004	215.8614	3.21013E+004
2	92	1.79493E+004	37.0925	2.35979E+004
3	118	1.79965E+004	24.8074	1.95063E+004
4	152	1.76086E+004	17.0392	1.83872E+004
5	195	1.75794E+004	15.3782	1.77829E+004
6	248	1.75458E+004	13.0863	1.83091E+004
7	318	1.75633E+004	12.9761	1.86488E+004
8	408	1.74944E+004	12.4121	1.94266E+004
9	526	1.74697E+004	10.0461	2.06047E+004
10	676	1.74533E+004	9.1596	2.09136E+004

(c)

Fig 4: (a) Axi-symmetric model (b) discretized with triangular elements and (c) convergence data of a coaxial coils in free air.

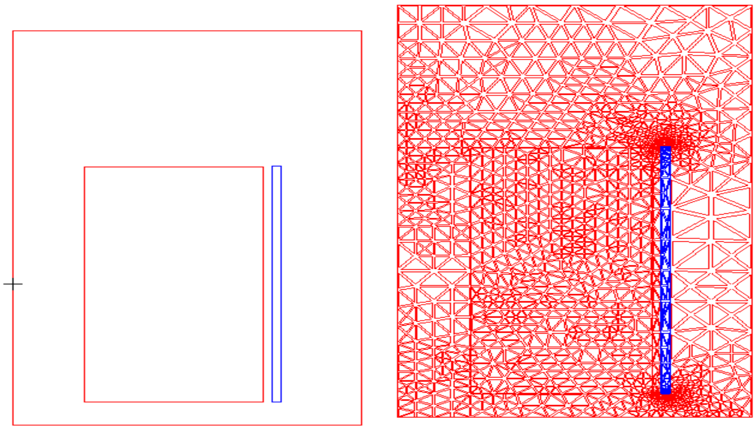

(a) (b)

CONVERGENCE DATA

Number of passes:

Completed 13

Remaining 0

Convergence criteria:

Target Error: 1%

Energy Error: 1.25%

Delta Energy: 0.0242%

Pass	Triangles	Total Energy(J)	Energy Error(%)	Mag Force(N)
1	55	2.61803E-001	26.4513	4.70441E-001
2	153	2.66075E-001	5.4982	4.47281E-001
3	196	2.66577E-001	4.3881	4.14245E-001
4	254	2.67795E-001	3.8815	4.12048E-001
5	326	2.68335E-001	3.0087	4.80216E-001
6	421	2.68882E-001	2.6847	4.91555E-001
7	541	2.68103E-001	2.4064	4.53404E-001
8	701	2.68483E-001	2.3349	4.77648E-001
9	905	2.68680E-001	2.1226	4.79668E-001
10	1170	2.68824E-001	2.0687	4.98732E-001
11	1513	2.68735E-001	1.5829	4.94284E-001
12	1955	2.68504E-001	1.4868	4.90424E-001
13	2532	2.68439E-001	1.2525	5.04284E-001

(c)

Fig 5: (a) Axi-symmetric model (b) discretized with triangular elements and (c) convergence data of a single coil with permanent magnet in free air.

Table 1. Standard layout in a Terfenol-D actuator

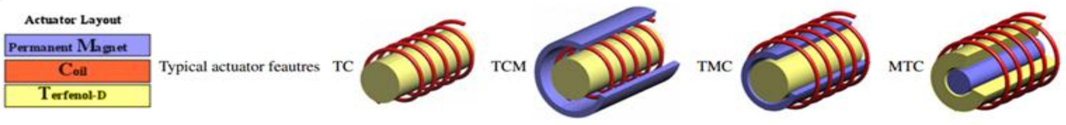

Magnetic bias with	DC coil	Permanent magnets		
Magnetic bias level	Low	Medium	Medium, high	High
Terfenol-D shaped	Rod, bar	Rod	Rod	Hollow rod
Structure	Simple	Medium	Medium	Complex

Table 2. Reluctance of components of a Terfenol-D actuator

Name of component	Length of component (m)	Diameter of component (m)	Area of component (m^2)	Reluctance of component (AT/Wb)
Terfenol-D	0.08	0.025	4.9×10^{-4}	3.2×10^{7}
Plunger	0.035	0.031	7.5×10^{-4}	9225.4
Top end plate	0.067	-	2.1×10^{-3}	63332.6
Top end plate edge	0.032	-	3.4×10^{-3}	1890.3
Housing	0.083	-	3.4×10^{-3}	4903.02
Bottom end plate edge	0.025	-	3.4×10^{-3}	147.7
Bottom end plate	0.067	-	1.05×10^{-3}	12665.15
Bottom support of Terfenol-D	0.025	-	4.9×10^{-4}	1013.2
$\Re_{Total} = 3.24\times10^{7}$ AT/Wb				